Effect of phytoliths for mitigating water stress in durum wheat

Jean-Dominique Meunier, Doris Barboni, Muhammad Anwar-Ul-Haq, Clément Levard, Perrine Chaurand, Vladimir Vidal, O. Grauby, Roland Huc, Isabelle Laffont-Schwob, Jacques Rabier, et al.

Jean Dominique Meunier[1], Doris Barboni[1], Muhammad Anwar-ul-Haq[2], Clément Levard[1], Perrine Chaurand[1], Vladimir Vidal[1], Olivier Grauby[3], Roland Huc[4], Isabelle Laffont-Schwob[5], Jacques Rabier[5] and Catherine Keller[1]

[1]CNRS, IRD, Coll France, CEREGE, Aix Marseille Université, 13545 Aix-en-Provence Cedex 04, France; [2]Institute of Soil & Environmental Sciences, University of Agriculture, 38040 Faisalabad, Pakistan; [3]CINaM, CNRS, Aix Marseille Université, Campus de Luminy Case 913, 13288 Marseille Cedex 9, France; [4]Unité Ecologie des Forêts Méditerranéennes (URFM), INRA, Domaine Saint Paul, Site Agroparc, 84914 Avignon Cedex 9, France; [5]CNRS, IRD, IMBE, Avignon University, Aix Marseille Université, Case 4, 3 Place Victor Hugo, 13331 Marseille Cedex 03, France

Author for correspondence:
Jean Dominique Meunier
Tel: +33 4 42 97 15 26
Email: meunier@cerege.fr

Received: *13 November 2016*
Accepted: *28 February 2017*

New Phytologist (2017) **215:** 229–239
doi: 10.1111/nph.14554

Key words: drought, phytolith, trichome, wheat, X-ray imaging.

Summary

- The role of silicon (Si) in alleviating biotic and abiotic stresses in crops is well evidenced by empirical studies; however, the mechanisms by which it works are still poorly known. The aim of this study is to determine whether or not phytolith composition and distribution in wheat are affected by drought and, if so, why.
- Durum wheat was grown using hydroponics in the presence of polyethylene glycol (PEG)-6000 to perform a water-stress simulation. We developed an original method for *in situ* analysis of phytoliths in leaves via X-ray imaging.
- PEG was efficient in inhibiting water uptake by roots and creating stress, and prevented a small fraction of Si from being accumulated in the shoots. The application of Si with PEG maintained shoot and root fresh weights (FW) and relative water content at higher values than for plants without Si, especially at PEG 12%.
- Our data show that, under water stress in the presence of Si, accumulation of phytoliths over the veins provides better support to the leaf, thus allowing for a better development of the whole plant than in the absence of Si. The development of silicified trichomes in durum wheat depends primarily on the availability of Si in soil and is not an adaptation to water stress.

Introduction

Drought stress is of increasing concern because its impact on crop production is expected to increase as a result of global warming (Tubiello *et al.*, 2007). One approach to mitigating the effect of global warming on crop production is to select crops adapted to water shortage. In this regard, it is required that we improve our knowledge on the interactions between plants and soil (Velde & Barré, 2010), and more specifically on the role of elements (such as silicon, Si) that have been neglected in the past. Silicon, the most common element in the Earth's crust after oxygen, accumulates highly in the shoots of many terrestrial plants (1–10% DW), particularly monocots (Hodson *et al.*, 2005). Silicon generally is not considered as an essential nutrient but is often beneficial for crops under biotic and abiotic stresses (Ma, 2004; Sacala, 2009; Guntzer *et al.*, 2012; Zhu & Gong, 2014; Keller *et al.*, 2015; Rizwan *et al.*, 2015).

The amount of Si/phytoliths (microscopic particles of silica formed in living plants) accumulated in plants depends on water and soil Si availability (Jones & Handreck, 1965; Ma & Takahashi, 2002; Dietrich *et al.*, 2003; Henriet *et al.*, 2008; Melzer *et al.*, 2012; Gocke *et al.*, 2013; Quigley & Anderson, 2014), plant taxa (Hodson *et al.*, 2005; Ma & Yamaji, 2008; Cornelis *et al.*, 2011; Katz *et al.*, 2013) and environmental factors such as grazing (McNaughton *et al.*, 1985; Melzer *et al.*, 2010; Garbuzov *et al.*, 2011; Cooke & Leishman, 2012; Soininen *et al.*, 2013; Hartley *et al.*, 2015) or temperature (Dey *et al.*, 2015). It has been shown that silica concentration is significantly correlated with transpiration rates (Jones & Handreck, 1965; Hutton & Norrish, 1974; Euliss *et al.*, 2005; Faisal *et al.*, 2012), although the active uptake of Si may not allow for a direct quantification of transpiration (Jarvis, 1987; Mayland *et al.*, 1991; Gocke *et al.*, 2013).

The beneficial effect of Si for plants affected by drought stress is still not well established and appears to be involved in improving water status, osmotic adjustment, photosynthesis, antioxidant defense and the balance of nutrient uptake (Gong *et al.*, 2003; Hattori *et al.*, 2005; Eneji *et al.*, 2008; Zhu & Gong, 2014).

The role of Si in alleviating water stress can be further assessed by the analysis of Si deposited in the plants as phytoliths. Si deposited beneath the leaf cuticle forms a Si-cuticle double layer that may decrease transpiration in rice (Yoshida *et al.*, 1962; Ma, 2004). When drought-stress increases, grasses also accumulate more Si in their leaf epidermis, particularly in the bulliform (motor) cells (Issaharou-Matchi *et al.*, 2016). In paleoclimatological studies, the relative abundance of silicified bulliform cells is used to infer aridity (Bremond *et al.*, 2004; Novello *et al.*, 2012). However, other studies showed that the silicified bulliform cells

are favored when transpiration is high (Takeoka *et al.*, 1984) or simply when the Si content in soils is high (Fernandez Honaine & Osterrieth, 2012). According to Takeda *et al.* (2013), silicified trichomes could efficiently help plants to absorb visible light. Waterkeyn *et al.* (1982) suggested that silicified trichomes are areas of intense transpiration and may thus contribute to cooling plants; however, this remains speculative (Hodson *et al.*, 1985; Kaufman *et al.*, 1985). Issaharou-Matchi *et al.* (2016) showed that in the drought-adapted grass *Pennisetum pedicellatum* growing in South Niger, the amount of silicified trichomes remained unchanged despite increasing drought stress. Therefore, the role of phytolith morphotypes in alleviating drought stress remains controversial.

In order to determine if plants develop specific phytolith distribution under drought stress, we conducted hydroponic experiments using polyethylene glycol (PEG)-6000 for simulating water stress at the root level (Kaufmann & Eckard, 1971). Durum wheat was considered here because it is widely cultivated in dry climate areas. We monitored the growth and physiological parameters that may be affected by drought and assessed the putative role of silicon application for mitigating the impact of drought. We analyzed phytolith morphotypes under an optical microscope after a wet extraction/acid digestion, and we performed *in situ* analysis of phytoliths in leaves via X-ray imaging: combining 2D chemical mapping using micro X-ray fluorescence spectroscopy (micro-XRF) and 3D imaging using X-ray computed tomography (CT).

Materials and Methods

Experimental layout

Durum wheat variety Claudio (*Triticum turgidum* subsp. *durum* cv Claudio W.) was used as a test case against the application of silicon as silicic acid neutralized by KOH (Rizwan *et al.*, 2016) and polyethylene glycol (PEG)-6000 for water stress and grown in hydroponics in controlled conditions. PEG-6000 (VWR Chemicals, Strasbourg, France) was used to develop slight to moderate water stress with the addition of 6% and 12% PEG solution. The seeds were washed with distilled water, sterilized with a 2.6% solution of sodium hypochlorite for 3 min, and then washed again with distilled water for six to seven times to remove the excess chloride. The seeds were then imbibed for 4 h in water by maintaining aeration to avoid fermentation. After 4 h, the seeds were shifted to Petri dishes with filter paper. The seeds germinated after 5 d. The seedlings were then transferred in 12-l plastic buckets containing nutrient solution (KH_2PO_4, K_2HPO_4, $MgSO_4{\cdot}7H_2O$ 0.5 mM, KNO_3, Ca $(NO_3)_2{\cdot}4H_2O$ 1 mM, KCl 0.125 mM, H_3BO_3 50 µM, $MnSO_4{\cdot}H_2O$ 12 µM, $CuSO_4{\cdot}H_2O$ 0.7 µM, $ZnSO_4{\cdot}7H_2O$ 1 µM, $MoO_4Na_2{\cdot}2H_2O$ 0.25 µM, and FeIII-EDTA-Na 100 µM) prepared with Milli-Q (Millipore) water. There were six treatments: control, PEG 6%, PEG 12%, silicon (Si) 1.5 mM, Si 1.5 mM + PEG 6%, and Si 1.5 mM + PEG 12%. Additional potassium (K) produced by Si supplementation was subtracted from KNO_3 and the resultant nitrate loss was supplemented with dilute nitric acid. One hundred plants were maintained in each bucket with continuous aeration. These plants were grown for 30 d by maintaining a short day duration of light 8 h : 16 h, day : night at 187 µmol photon $m^{-2}\,s^{-1}$ light intensity. The pH was adjusted to 6.5 ± 0.5 daily with 1 mM 2-morpholinoethanesulphonic acid (MES) buffer. Aeration was maintained via an aeration pump. Nutrient solutions were changed every 3 d during the first 10 d and every 2 d during the remaining 20 d.

Analyses of plants

The root and shoot fresh weight (FW) were measured on 17–20 selected plant replicates. Technical problems precluded the measurements of dry weight (DW). The values of the predawn leaf water potential (LWP) were measured on leaf blades using a Scholander-type pressure chamber. The measurements were made on one leaf per seedling and five to six seedlings per treatment at the end of the night period. The fully expanded younger leaves were also collected ($n = 4$) to measure relative water content (RWC) according to Weatherley (1950):

$$\mathrm{RWC} = \frac{(\mathrm{FW} - \mathrm{DW})}{(\text{turgid weight} - \mathrm{DW})} \times 100.$$

Plants were oven-dried at 70°C and DW was recorded when constant weight was reached. The turgid weight was obtained by dipping a leaf in water for 4 h at room temperature, followed by weighing the leaf and then drying it at 70°C for 72 h. Phytometabolites were monitored using nondestructive Multiplex® (Orsay, France) equipment that uses fluorescence technology with multiple excitations to measure chlorophyll and phenolic compound indices. Only the simple fluorescence ratio under red (SFR_R) excitation was retained to estimate the chlorophyll content of seedlings just before harvest. The results are expressed as a mean of 18 measurements per condition in Multiplex units.

The Si concentration of shoots was determined using 1% Na_2CO_3 extraction at 85°C (Meunier *et al.*, 2014). Approximately 30 mg of dried plant material were mixed with 40 ml of 1% Na_2CO_3 solution in a polypropylene bottle and placed in a shaker bath at 85°C and 100 rpm. In principle, all of the Si is dissolved after 1 h. A 1-ml aliquot was removed after 3, 4 and 5 h from each sample bottle and placed into pre-labelled 22-ml scintillation vials containing 9 ml of a solution of 0.021 N HCl to neutralize Na_2CO_3. Dissolved Si (DSi) was obtained by the molybdenum blue colorimetric method using Spectroquant® reactants manufactured by Merck (Fontenay sous Bois, France). Absorption was measured at 820 nm with a Jasco V-650 spectrometer. Calibration lines ($R^2 > 0.999$) were done using dilute solutions from a standard Si solution at 1 g l^{-1} (PlasmaCAL). DSi was calculated by averaging the three values at 3, 4 and 5 h.

Phytoliths were extracted in six sets of plant samples, one from each treatment. Each set included five specimens, with each set treated together. Shoots only were analyzed after 30 d of growth, including all leaves and stems. Phytoliths were extracted using

concentrated HNO_3, $HClO_4$ and H_2O_2 at 50°C to destroy organic matter before observation and counting under optical microscope. Slides were prepared with Canada balsam, and then observations were conducted at × 500 magnification. Phytolith morphotypes were described following the international phytolith nomenclature (Madella *et al.*, 2005) and counted separately to evaluate the degree of silicification of different epidermal cells. In each slide, phytoliths were counted along five random lines, and the results were compared through statistical analysis.

All of the data were analyzed statistically using one-way ANOVA with XLSTAT (Addinsoft) at a significance level of $P < 0.05$ via the Tukey test.

In situ phytolith analysis

Leaves for 2D and 3D analyses were prepared using the critical point drying method following two steps: fixation and dehydration in a 2.5% glutaraldehyde solution buffered at pH = 7.2 in 0.1 M sodium phosphate, followed by soaking in concentrated solutions of ethanol (from Leica EM CPD300 Application Booklet 01/12); and supercritical drying using Leica EM CPD300°, which consists of the replacement of ethanol by CO_2 in the supercritical state. Silicon (Si) and calcium (Ca) were detected and mapped on dried leaf pieces using an X-ray analytical microscope (XGT-7000; Horiba, Kyoto, Japan) equipped with a focused X-ray source of 10 µm (Rh target, accelerating voltage of 15 kV, current 0.92 mA). Chemical maps of 256 × 256 pixels with a pixel size of 10 µm and a total counting time of 20 × 1000 s were recorded.

3D imaging was performed using both micro- and nano-X-ray computed tomography (micro- and nano-CT). Imaging of the leaves was performed using a microXCT-400 X-ray microscope (Zeiss Xradia). Scans were performed at 40 kV (W target) and 250 mA with 2001 projections (angle step of 0.18° from −180 to 180°) and a 10-s exposure time per projection for a total scan time of 6 h and 30 min. Data were acquired with a × 10 magnification optical objective. The isotropic voxel size achieved under these conditions was 1.77 µm, and the field of view (FOV) was $1.85 \times 1.85 \times 1.85\ mm^3$. A single trichome was imaged at the nanoscale using an UltraXRM-L200 X-ray microscope (Zeiss Xradia) equipped with a copper X-ray source (rotating anode). A total of 901 projections from −90 to 90° with an angle step of 0.2° were recorded, with an exposure time of 40 s per projection for a total scanning time of 12 h. This equipment provides 3D images with a unique resolution at the laboratory scale, that is, a voxel size of 63.5 nm, and an FOV of $65 \times 65 \times 65\ \mu m^3$. Reconstruction of the volume was performed with the XMRECONSTRUCTED-PARALLEL BEAM-9.0.6445 software using a Filtered Back Projection algorithm.

Data normalization and thresholding was performed using AVIZO 8.0 software (Hillsboro, OR, USA). First, histograms of the reconstructed volumes were extracted. These histograms represent the X-ray attenuation in each voxel (expressed as an arbitrary gray scale value, GSV) of the analyzed volume as a function of the number of voxels for each GSV (intensity). Normalization of the histograms was performed using air as an internal standard. This consisted of shifting and multiplying the histogram GSV axis by given factors so that all of the air contributions, fitted with a Gaussian function, overlap (same maximum position and full-width at half maximum). To obtain *in situ* 3D images of phytoliths, we compared the histograms of GSVs of leaves with and without Si, and the images obtained after treatment of the gray levels by AVISO; this comparison allowed for isolating phytoliths already recognized under the optical microscope and Micro-XRF 2D images. 2D and 3D analyses were completed by scanning electromicroscopy (SEM) at CEREGE (Hitachi S300N at 20 kV; Hitachi, Tokyo, Japan) and at the Centre Interdisciplinaire de Nanosciences de Marseille (CINaM, JEOL JSM-6320F at 15 kV).

Results and Discussion

Effect of PEG and Si on plant development

Compared with the control (no silicon, Si), application of polyethylene glycol (PEG) at both concentrations significantly decreased the shoot and root FW as well as relative water content (RWC) (Fig. 1). The chlorophyll index and leaf water potential (LWP) were reduced as well, but only significantly with PEG12%. PEG was therefore efficient in inhibiting water uptake by roots and creating stress. Our results are in broad agreement with previous studies (Kaufmann & Eckard, 1971; Chazen *et al.*, 1995; Pei *et al.*, 2010; Vijayakumari & Puthur, 2016). Application of Si to the control conditions (no PEG) had no significant effect on FW, LWP, RWC and chlorophyll content, but led, as expected, to a greater Si concentration in the shoots (Fig. 1). Silicon concentrations measured in the shoots (1.5–1.7% DW) fall within the range of values obtained from previous studies of wheat grown hydroponically (Rizwan *et al.*, 2016) and in fields (Merah *et al.*, 1999), and within the range of values obtained for Poales (Hodson *et al.*, 2005). Drought stress induced by PEG led to a low but significant decrease in Si concentration (from 1.7 to 1.3–1.2% wt). Silicon application did not improve LWP (PEG12% and Si+PEG12% treatments led to similar values *c.* −3.3 MPa), but it allowed RWC to remain at *c.* 60%, despite PEG treatments. Hence, PEG prevented a small fraction of Si from being accumulated in the shoots. The addition of Si is therefore likely to limit transpiration, as shown by previous studies (Gao *et al.*, 2006; Saud *et al.*, 2014).

The Si concentration in plants where Si was not applied (with PEG or not) was not null, suggesting contamination during the experiment. This contamination probably originated from the chemical products and glassware used for the preparation of the nutritive solution. The total lack of Si in the plants would have suggested that Si is not an essential nutrient for the growth of these varieties. However, the only inference we can make is that the addition of Si to the nutrient solution did not affect plant development when water and nutrients were not limiting factors.

Silicon application in the nutrient solution provides some evidence that Si mitigates the effect of water stress by improving shoot and root development, and water uptake and retention in the leaves of durum wheat, in agreement with previous studies

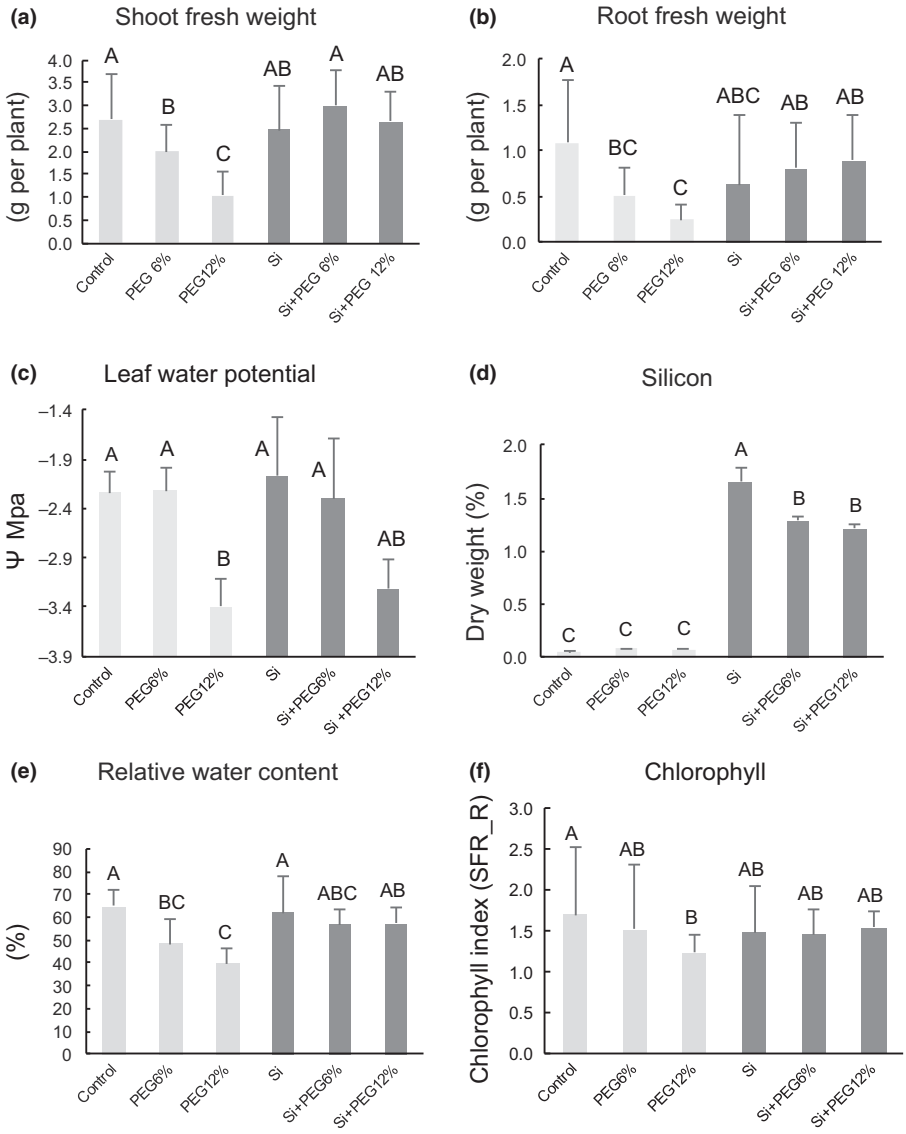

Fig. 1 Mean values for (a, b) growth parameters, (d) silicon (Si) content, (c, e) leaf water parameters and (f) chlorophyll index of durum wheat (*Triticum turgidum* subsp. *durum* cv Claudio W.) subjected or not to polyethylene glycol (PEG) and Si treatments. Error bars (only the upper limit is shown) represent +1 SD. Different letters indicate that the means are statistically different at the $P \leq 0.05$ level.

(Gong *et al.*, 2003; Ahmad *et al.*, 2007; Pei *et al.*, 2010; Sonobe *et al.*, 2011). The mechanism by which Si increases root water uptake is not well known and may imply a change in hydraulic conductivity and/or osmotic adjustment in the roots, as well as possible regulation by gene expression (Liang *et al.*, 2015; Exley, 2016; Shi *et al.*, 2016). Drought stress also affected photosynthetic pigments, as observed by Barbosa *et al.* (2015), implying that Si application significantly improved the functioning of the photosynthetic machinery, contributing to a better plant growth (e.g. Rizwan *et al.*, 2015).

Insights from the micro-XRF and CT imaging results

Histograms of Si-treated samples from the micro X-ray fluorescence spectroscopy (micro-XRF) and X-ray computed tomography (CT) images showed a large contribution at the highest gray scale value (GSV) (Fig. 2). This contribution does not appear on the histograms of Si-free samples. Voxels with the highest GSV, corresponding to the denser parts of the leaves, are then attributed to Si. The distribution of the denser voxels was fitted using the Gaussian curve Gauss 4 in Fig. 2. Three other Gaussian curves were required to fit the remaining GSV corresponding to air and plant material. The threshold value allowing the visualization of Si was set at the intersection between the Gauss 3, attributed to the plant material, and Gauss 4, attributed to Si. The distribution of voxels isolated from the thresholding procedure (attributed to phytoliths) was similar to the Si distribution in the leaf obtained by micro-XRF (Figs 3, 4). Calcium-rich spots (Fig. 3, green pixels) observed by micro-XRF were not visualized by micro-CT. The comparison of the 2D chemical map and 3D image of the same sample region validates the thresholding procedure determined to isolate and visualize phytoliths. Micro-XRF 2D images therefore provide evidence that silicification occurred essentially in the costal areas over the veins and as isolated trichomes (Figs 3, 4). Nano-CT images showed that silica in durum wheat leaves was also deposited as a thin silica layer, cementing cells of the epidermis (Fig. 5) sometimes embedded with trichomes.

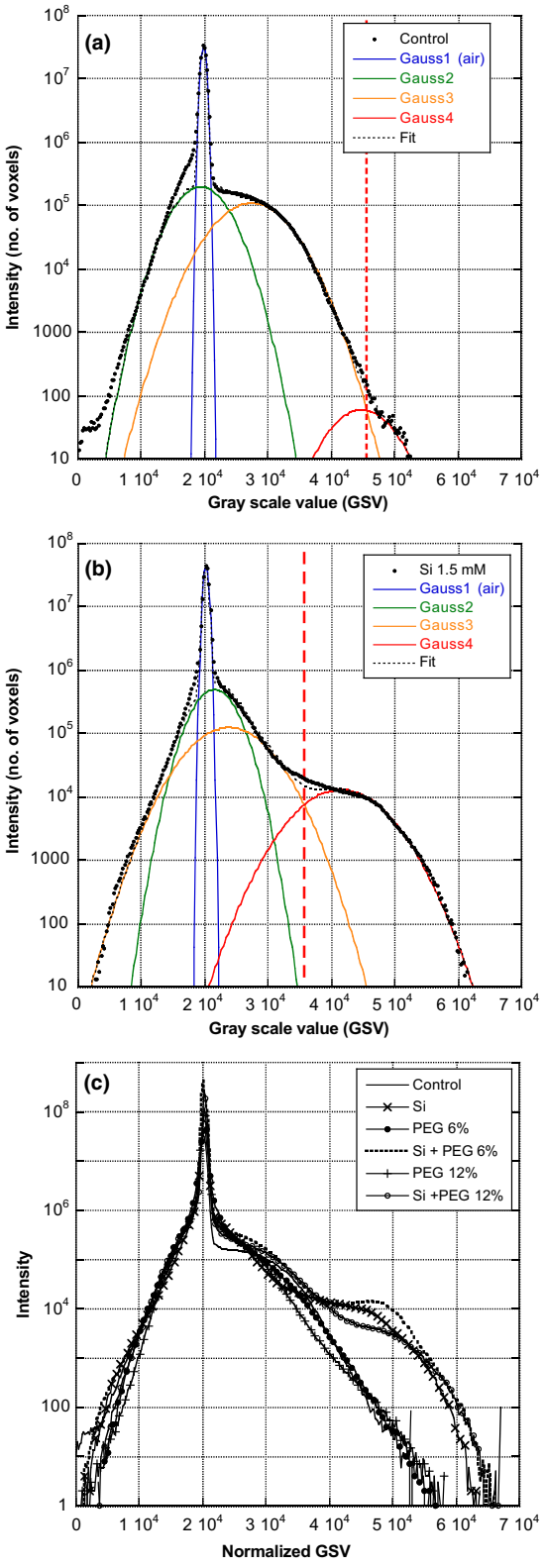

Fig. 2 Distribution of gray scale values (GSV) from the micro-computed tomography (micro-CT) images: fit of micro-CT normalized histograms of (a) a control leaf and (b) a leaf treated with silicon 1.5 mM, with four Gaussian curves. Each curve is attributed to a material in the sample, with a given X-ray attenuation. Gauss1 represents voxels of air; Gauss4 represents the denser voxels with higher X-ray attenuation, attributed to phytoliths. The threshold value used to isolate phytolith voxels (red frame) was selected at the intersection of curves Gauss3 and Gauss4. Similar fits were obtained for leaves treated with polyethylene glycol (PEG) 6%, and PEG 12%. (c) Normalized histograms of reconstructed volumes obtained by micro-CT for leaves with the six sets of treatment. The normalization procedure was based on the superimposition of the full-width at half maximum (FWHM) and the maximum position of all Gauss1 (air) functions. Si, silicon.

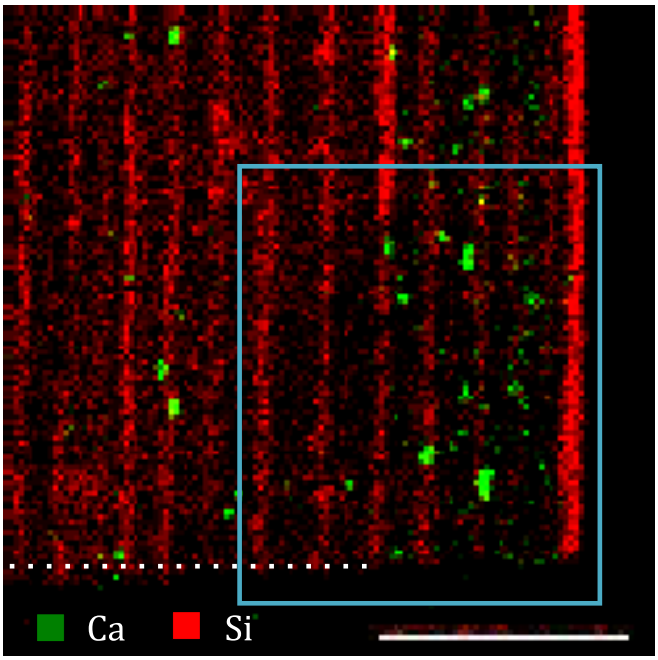

Fig. 3 Micro X-ray fluorescence spectroscopy (micro-XRF) (1 px = 20 µm, field of view (FOV) = 2.56 × 2.56 mm^2) 2D imaging of a dried leaf treated with silicon 1.5 mM (bar, 1000 µm) showing the distribution of silicon (Si) (red) and calcium (Ca) (green); the square is the position of the micro-computed tomography (micro-CT) image shown in Fig. 4(b).

Distribution of phytoliths in the leaves

As expected, without Si treatment, plants produced very few phytoliths, and proper counting could not be conducted under the microscope. Plants that received Si treatment, on the contrary, produced enough silica bodies and > 1000 phytoliths could be counted for each Si treatment (Si, Si+PEG6%, and Si+PEG12%) (Table 1). Silica bodies originating from cells of the upper epidermis, such as crenate and rondel morphotypes from silica cells (20–100 µm long, typical for Pooideae, Twiss *et al.*, 1969), elongate smooth and sinuate bodies from long cells (20–100 µm long), silica casts of trichomes (10–40 µm long) and trichome base cells, are the most abundant phytoliths, whereas phytoliths from parenchyma/collenchyma cells (mainly blocky bodies) are rare (Table 1; Fig. 6). This pattern is common in grasses (e.g. Hodson & Sangster, 1988; Ma & Takahashi, 2002). The microscopic analysis of the phytolith particles in plants that received Si application shows that silicification in durum wheat leaf blades

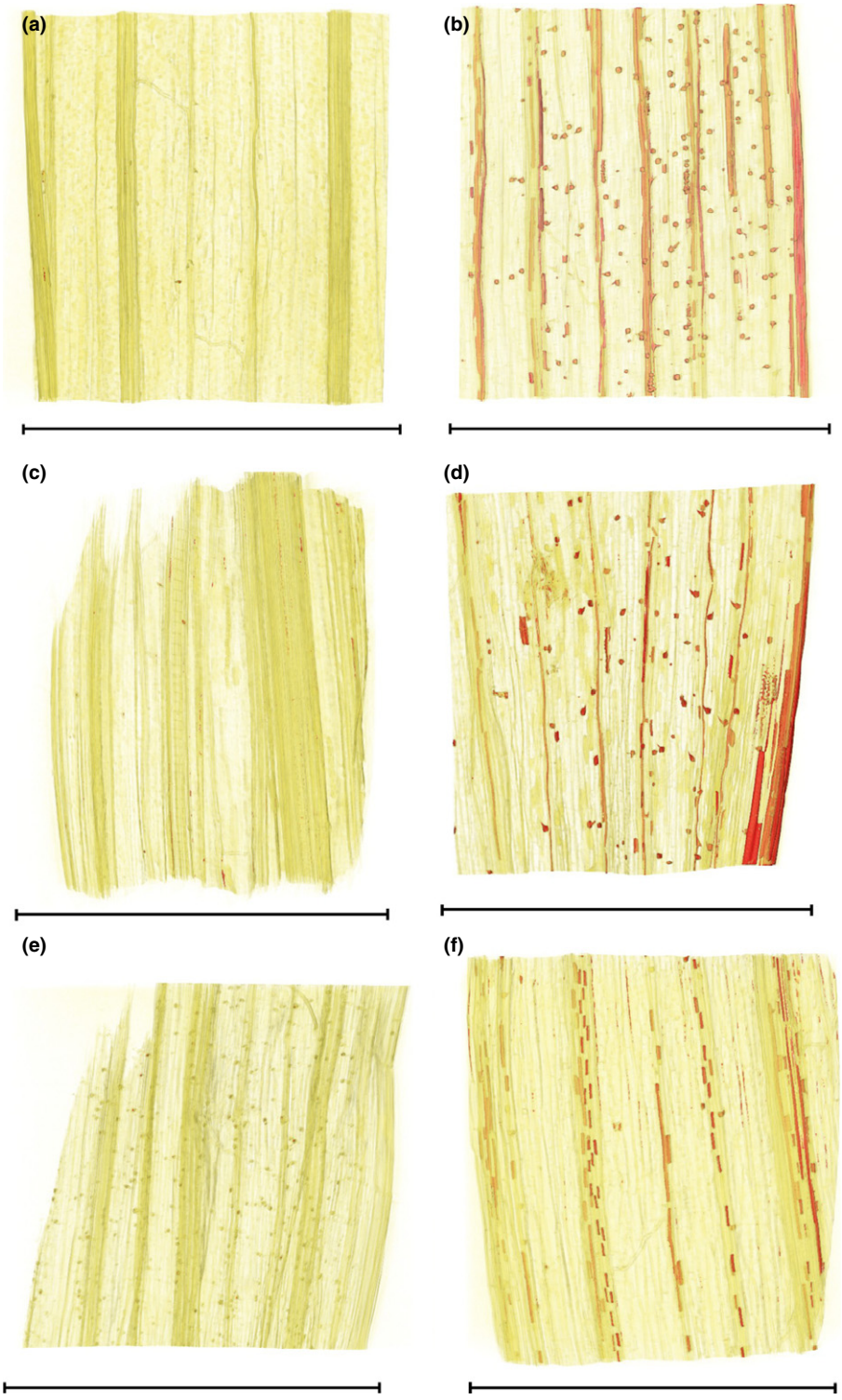

Fig. 4 Volume renderings of reconstructed micro-computed tomography (micro-CT) images of (a) a control leaf, a leaf treated with (b) silicon 1.5 mM, (c) polyethylene glycol (PEG) 6%, (d) silicon 1.5 mM + PEG 6%, (e) PEG 12% and (f) silicon 1.5 mM + PEG 12%. Thresholded voxels, attributed to phytoliths, are false-colored in red (surface rendering). Bars, 1500 μm.

barely occurred in internal tissues but was important in the epidermis, particularly in the costal areas, in good agreement with the micro-XRF and micro-CT imaging. Surprisingly, we observed no cuneiform phytoliths originating from bulliform cells. Silicification of bulliform cells is common in wheat leaves (Hodson & Sangster, 1988) but may require > 30 d of growth to produce phytoliths (Motomura *et al.*, 2004).

Silica layers observed under nano-CT imaging (Fig. 5) were interpreted to be similar to plate fragments of 1- to 4-μm thick and some hundreds of micrometers in width under an optical microscope (Fig. 6). The relative abundance of the plate fragments observed during phytolith analysis cannot be used to infer the importance of the extracellular silica sheet because fragmentation may have occurred during phytolith extraction. The extent

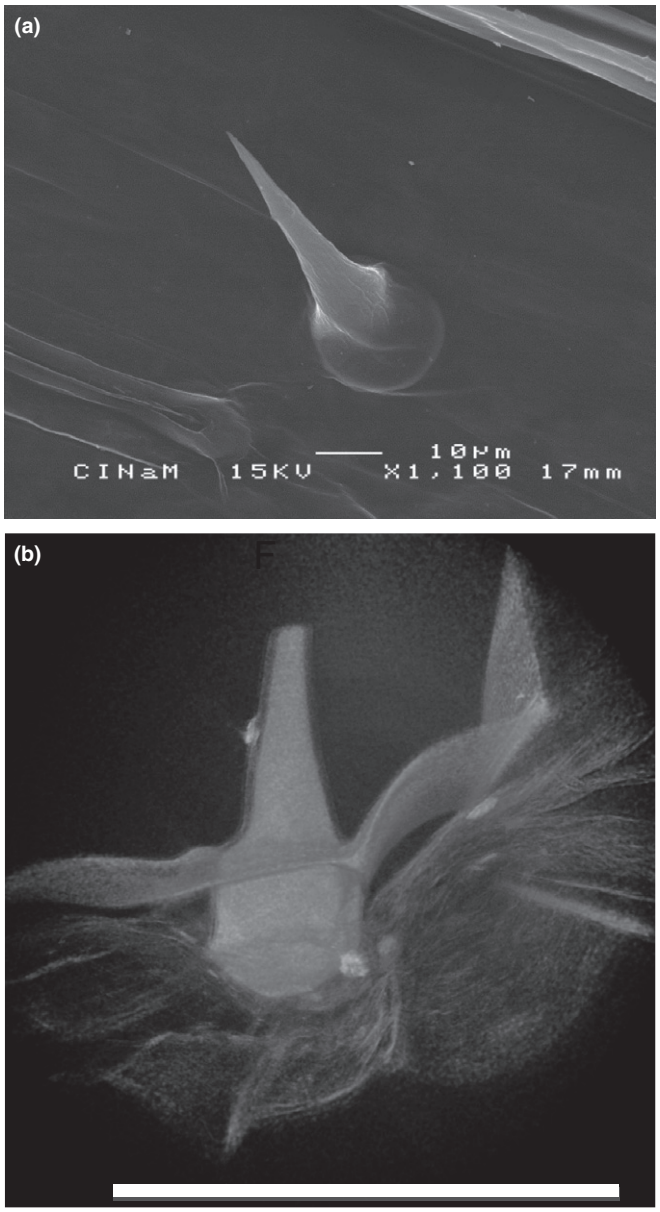

Fig. 5 Magnified view of trichomes from (a) a leaf without silicon (Si) treatment in scanning electromicroscopy (SEM); Energy dispersive spectroscopy (EDS) spectra (not shown) showed that Si is present but not as dominant as is the case for silicified trichome; (b) a leaf treated with silicon 1.5 mM observed using nano-X-ray computed tomography (nano-CT) (voxel size of 63.5 nm): volume rendering of the reconstructed volume (bar, 50 µm).

of these plates over the leaf blade is not visible either on the micro-CT images because of the image resolution (1 vx = 1.76 µm, which is comparable to the thickness of the silica layer of only 1–1.3 µm) and/or because of the likely low density of the silica layer. It was not possible, therefore, to evaluate differences between treatments, if any, in the silica cuticle layer structure in durum wheat leaves. Plates are interpreted to be similar to the cuticle layers observed in the inflorescence bracts for the drought-adapted grass *Phalaris* in various British grass genera and some cereals (Wynn Parry & Smithson, 1964) and in rice (Yoshida *et al.*, 1962). In the husk epidermis of rice, the silica layer is as thick as 20–30 µm (Yoshida *et al.*, 1962; Gu *et al.*, 2013). This silica layer superimposed over the epidermis below the (organic) cuticle likely constitutes a continuous external layer that can prevent fungal penetration and/or transpiration through the epidermis (see review in Liang *et al.*, 2015).

Distribution of phytoliths and water stress

With PEG 6%, silica deposits were discontinuous in the costal areas and silicified trichomes were scarce on the epidermis (Fig. 4d). With PEG 12%, silicification was even weaker and restricted to the costal areas, where crenate silica bodies form dashed lines and silicified trichomes were barely visible (Fig. 4f). A simple counting of trichomes from the micro-CT images showed that the density of silicified trichomes decreased from 51 mm^{-2} under nondrought condition (+Si) to 21 mm^{-2} under Si+PEG 6% and 5 mm^{-2} under Si+PEG 12% (Table 2). The decrease in trichome number in leaves with PEG treatments was not reflected by the relative abundance of phytolith morphotypes, as obtained by counting under the microscope (Table 1). This is likely because phytolith countings did not take into account the decrease in Si content in leaves with PEG treatments. In all PEG treatments, trichomes were less abundant than the silica cells present all over the veins (Table 1); thus, during PEG treatments, trichomes were more affected than the silica cells. Therefore, under drought conditions, silicification would have become restricted to the silica cells over the veins and silicified trichomes did not appear as an indicator of water stress.

Trichomes are common in silicified plant cells in grasses (Mulholland & Rapp, 1992), including durum wheat (Kaplan *et al.*, 1992). They constitute one of the initial stages of silicification in grasses (Kaufman *et al.*, 1981; Sangster *et al.*, 1983; Motomura *et al.*, 2006). For example, de Souza *et al.* (2014) found that soybean treated with silica showed an increase in trichome density, thereby contributing to the defense against insects. The addition of Si to hydroponic nutrient media increased resistance of cucumber to powdery mildew, where silica accumulation was restricted to trichomes (Samuels *et al.*, 1993). Here, we did not observe the development of silicified trichomes as a defense against stress, contrary to the results in the literature.

Trichomes also were detected in leaves from plants where Si was not applied (–Si), but they were difficult to count using micro-CT images because of their small size and their lack of Si content. Such nonsilicified trichomes were not detected in leaves treated with Si. Using Energy Dispersive Spectroscopy (EDS) under SEM, these (–Si) trichomes (Fig. 6) were found to contain Si in low amount (data not shown), as observed in the bulk (Fig. 1). The counting using SEM images showed that (–Si) trichomes were rare on the leaf blade in the control plants (density of 0.3 mm^{-2} calculated from a count of two non-Si trichomes on a leaf surface of 7.1 mm^2), whereas they were more abundant under drought conditions (1.5 mm^{-2} at PEG 12% as 15 trichomes counted on 9.8 mm^2). The increase in (–Si) trichomes in the PEG 12% treatment (Table 2) may indicate a reaction to water stress, but more measurements are required. There is good

evidence that trichomes, for example, without any reference to their Si content play a role as a defense against herbivory (Dalin *et al.*, 2008). Leaf pubescence is also documented to be an adaptation to aridity (Johnson, 1975; Ehleringer & Mooney, 1978; Sandquist & Ehlinger, 1998; Benz & Martin, 2006), although the exact mechanisms are still to be understood. Wellso

Table 1 Relative abundance (in % relative to total phytolith sum) of phytolith morphotypes obtained from durum wheat (*Triticum turgidum* subsp. *durum* cv Claudio W.) plants (shoots only) grown under silicon (Si), Si+PEG6% and Si+PEG12% treatments

	Si		Si+PEG6%		Si+PEG12%	
Total counts	2116		1898		1351	
Phytolith morphotypes			%			
Sub-cuticular						
Plate (2–4-μm thick silica layer, may be several hundred micrometers wide)	23.7	C	16.3	CDE	22.2	CD
Upper epidermis						
Silicified trichome (tip and tip+base)	6.8	EFG	5.8	FG	6.0	EFG
Silicified epidermal tissue (multicellular) and stomata	1.3	G	0.3	G	0.4	G
Crenate bodies from silica cells	48.1	B	56.5	A	54.3	AB
Rondel (oblong bodies) from silica cells	2.5	G	1.3	G	2.4	G
Elongate smooth or sinuate body from long cells	13.6	DEF	14.5	DE	10.9	DEGF
Parenchyma/Collenchyma						
Blocky bodies (parallepipedal)	2.6	G	0.8	G	1.4	G
Unkown anatomical origin						
Irregular bodies with angular edges (sclereids?)	0.4	G	0.9	G	0.1	G
Unidentified silica bodies	2.2	G	2.4	G	2.5	G

Different letters indicate that the means are statistically different at $P \leq 0.05$ level. PEG, polyethylene glycol.

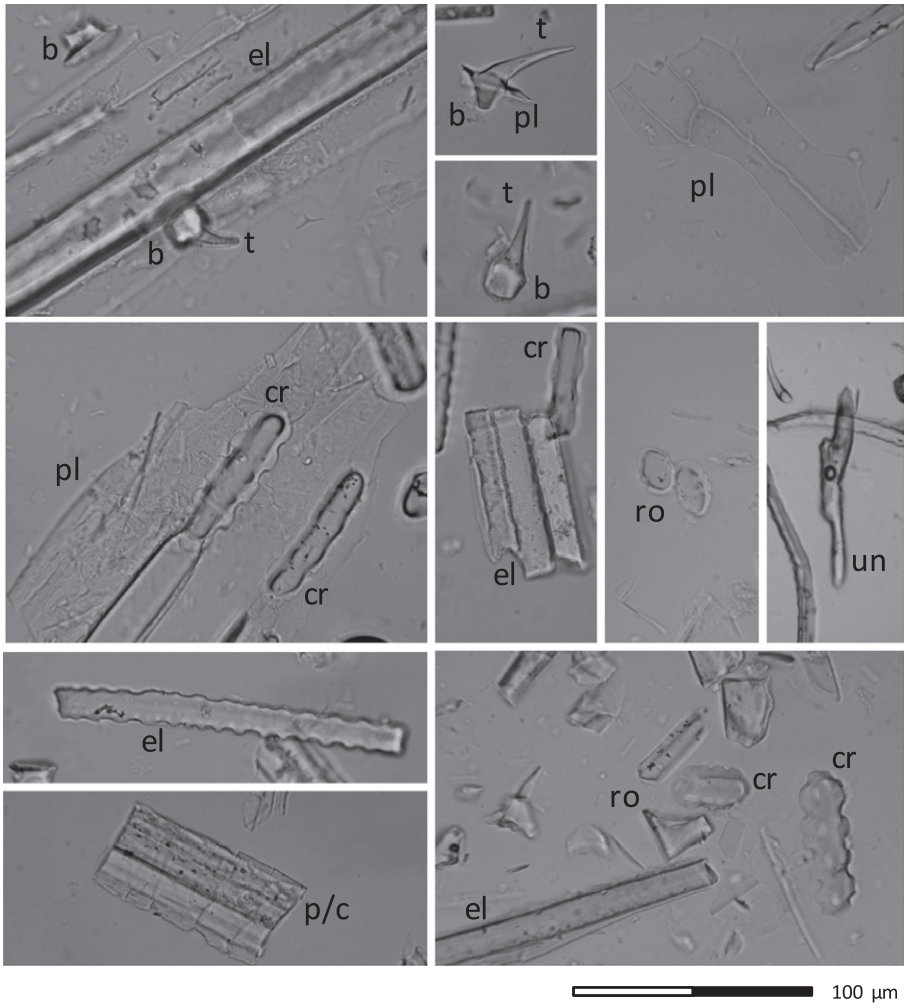

Fig. 6 Micrographs of phytoliths extracted from the leaves of durum wheat (*Triticum turgidum* subsp. *durum* cv Claudio W.). Phytoliths shown here are silicified trichomes (b, base of trichome; t, trichome), silicified epidermal short cells (ro, rondel; cr, crenate), silicified epidermal long cells (el, elongate smooth or with sinuous edges), fragments of the silica layer (pl, plate), and silicified parenchyma or cork tissue fragments in strand (p/c); un, unidentified silica bodies.

Table 2 Density of trichomes on the leaf epidermis of durum wheat (*Triticum turgidum* subsp. *durum* cv Claudio W.) specimens grown under different treatments

Treatment	Density of silicified trichomes on the leaf epidermis (nb mm^{-2})	Density of non silicified trichomes on the leaf epidermis (nb mm^{-2})
Control		0.3
Control+PEG 12%		1.5
Si 1.5 mM	51	
Si 1.5 mM + PEG 6%	21	
Si 1.5 mM + PEG 12%	5	

Silicified trichomes were counted using micro-computed tomography (micro-CT) images, and nonsilicified trichomes were counted using scanning electromicroscopy (SEM) images. Si, silicon; PEG, polyethylene glycol.

& Hoxie (1982) showed that the density of trichomes is positively correlated with temperature and negatively correlated with soil moisture in wheat grown in a growth chamber.

Beemster & Masle (1996) analyzed the effects of soil resistance to root penetration on the distribution of leaf cells in wheat (*Triticum aestivum*) and found that stressed roots led to an increase in the proportion of trichomes on the leaves. Doroshkov *et al.* (2011) showed that leaf trichomes are different from a given cultivar of wheat grown in a glasshouse and in field conditions: in the field, trichomes are more abundant and shorter than the ones found on wheat grown in controlled conditions, and those characteristics are attributed to adaptation to the more severe field conditions.

For the first time, here we have considered the silicification of trichomes as well as the trichome density as a plant response to drought stress (applied at the root level). The results of the present study may not be apparently in agreement with the literature, where the increase in trichome density is commonly interpreted as a response to plant stress. However, here, we show that trichomes may be silicified or nonsilicified and that they probably do not play the same role, if any, in the plant. In contrast to the conclusions found in the literature, the formation of silicified trichomes cannot be interpreted here as an adaptation to water stress, but simply as resulting from Si bioavailability. Our results imply that if Si is less available for the plant, then silicification preferentially occurs over the veins and not in the trichomes. Veins are the principal avenues for the transportation of Si in the leaves (Whang *et al.*, 1998; Rudall *et al.*, 2014). Taking into account the benefit of Si for improving the growth of plants (Fig. 1), our results suggest that it is the phytoliths accumulated over the veins that are at the origin of the improvements and not the silicified trichomes. Accumulation of Si in phytoliths over the veins may provide support to the leaf, thus allowing for better interception of light and consequently a better photosynthesis (Kaufman *et al.*, 1985), as well as better water transport. Accordingly, the silicified trichomes, having no function of support, may act as a reservoir for the excess of Si once the cells above the veins are filled. The storage function of trichomes also was suggested by Balestri *et al.* (2014) for heavy metals in fern. This effect may be useful for documenting the variability of Si concentration as a function of climatic parameters including aridity or evapotranspiration. Indeed, our results are in good agreement with those of Fernandez Honaine & Osterrieth (2012) in that the Si content and phytolith distribution are mainly controlled by Si availability. Thus, the use of phytolith types as indicators of aridity or other paleoenvironmental conditions should be evaluated carefully.

Conclusion

Our experiments have shown that the simulation of water stress by PEG addition has affected the development of durum wheat. Although the water stress applied was moderate (not all growth parameters were affected), Si was efficient at mitigating the early negative effect of drought. PEG affected not only the concentration of Si in the shoots, but also its distribution by limiting the formation of silicified trichomes. The mitigating effect of Si was attributed to the reinforcement of the structure of leaves through the preferential phytolith accumulation above the veins. The development of silicified trichomes in durum wheat depends primarily on the availability of Si in soil and is not an adaptation to water stress.

Acknowledgements

The study was made possible through the financial support of FR ECCOREV (AO 2013), BIOSiSOL project ANR-14-CE01-0002 and a grant from the High Education Commission of Pakistan for M.A-u-H. The authors also gratefully acknowledge the support from the 'Investissements d'Avenir' French Government program of the French National Research Agency that funded the French X-ray CT platform Nano-ID (ANR-10-EQPX-39-01), and Fanny Paris (CEREGE), Yves Gally (CEREGE) and Stéphane Jézéquel (ARVALIS, Institut du Végétal) for their fruitful collaboration.

Author contributions

J.D.M., D.B. and C.K. planned, designed the research, wrote the manuscript and participated to the analysis of the data; M.A-u-H., C.L., P.C., V.V., O.G., R.H., I.F-S. and J.R. performed experiments, analyzed the data and participated in the writing of the manuscript.

References

Ahmad F, Rahmatullah , Aziz T, Maqsood MA, Tahir MA, Kanwal S. 2007. Effect of silicon application on wheat (*Triticum aestivum* L.) growth under water deficiency stress. *Emirat Journal of Food and Agriculture* **19**: 1–7.

Balestri M, Ceccarini A, Forino LMC, Zelko I, Martinka M, Lux A, Castignione MR. 2014. Cadmium uptake, localization and stress-induced morphogenic response in the fern *Pteris vittata*. *Planta* **239**: 1055–1064.

Barbosa MAM, da Silva MHL, Viana GDM, Ferreira TR, Figueredo de Carvalho Souza CL, Guedes Lobato EMS, da Silva Lobato AK. 2015. Beneficial repercussion of silicon (Si) application on photosynthetic pigments in maize plants. *Australian Journal of Crop Science* **9**: 1113–1118.

Beemster GTS, Masle J. 1996. Effects of soil resistance to root penetration on leaf expansion in wheat (*Triticum aestivum* L.): comparison, number and size of

epidermal cells in mature blades. *Journal of Experimental Botany* **47**: 1651–1662.

Benz BW, Martin CE. 2006. Foliar trichomes, boundary layers, and gas exchange in 12 species of epiphytoic *Tillandsia* (Bromeliaceae). *Journal of Plant Physiology* **163**: 648–656.

Bremond L, Alexandre A, Peyron O, Guiot J. 2004. Grass water stress estimated from phytoliths in West Africa. *Journal of Biogeography* **31**: 1–17.

Chazen O, Hartung W, Neulan PM. 1995. The different effects of PEG 6000 and NaCl on leaf development are associated with differential inhibition of root water transport. *Plant, Cell & Environment* **18**: 727–735.

Cooke J, Leishman MR. 2012. Tradeoffs between foliar silicon and carbon-based defences: evidence from vegetation communities of contrasting soil types. *Oikos* **121**: 2052–2060.

Cornelis JT, Delvaux B, Georg RB, Lucas Y, Ranger J, Opfergelt S. 2011. Tracing the origin of dissolved silicon transferred from various soil–plant systems towards rivers: a review. *Biogeosciences* **8**: 89–112.

Dalin P, Agren A, Björkmann C, Huttunen P, Kärkkäinen K. 2008. Leaf trichome formation and plant resistance to herbivory. In: Schaller A, ed. *Induced plant resistance to herbivory*. Dortrecht, the Netherlands: Springer Science+Business Media, 89–105.

Dey SB, Ghosh R, Shekhar M, Mukherjee B, Bera S. 2015. What drives elevational patterns of phytolith diversity in *Tysanolaena maxima* (Roxb.) O. Ktze? A study from the Darjeeling Himalayas. *Flora* **211**: 51–61.

Dietrich D, Hinke S, Baumann W, Fehlhaber R, Bäucker E, Rühle G, Wienhaus O, Marx G. 2003. Silica accumulation in *Triticum aestivum* L. and *Dactylis glomerata* L. *Analytical and Bioanalytical Chemistry* **376**: 399–404.

Doroshkov AV, Pshenichnikova TA, Afonnikov DA. 2011. Morphological characterization and inheritance of leaf hairiness in wheat (*Triticum aestivum* L.) as analysed by computer-aided phenotyping. *Russian Journal of Genetics* **47**: 739–743.

Ehleringer JR, Mooney HA. 1978. Leaf hairs: effects on physiological activity and adaptive value to a desert shrub. *Oecologia* **37**: 183–200.

Eneji AE, Inanaga S, Muranaka S, Li J, Hattori T, An P, Tsuji W. 2008. Growth and nutrient use in four grasses under drought stress as mediated by silicon fertilizers. *Journal of Plant Nutrition* **31**: 355–365.

Euliss KW, Dorsey BL, Benke KC, Banks MK, Schwab AP. 2005. The use of plant tissue silica content for estimating transpiration. *Ecological Engineering* **25**: 343–348.

Exley C. 2016. A possible mechanism of biological silicification in plants. *Frontiers in Plant Science* **6**: 853.

Faisal S, Callis KL, Slot M, Kitajima K. 2012. Transpiration-dependent passive silica accumulation in cucumber (*Cucumis sativus*) under varying soil solution availability. *Botany-Botanique* **90**: 1058–1064.

Fernandez Honaine M, Osterrieth ML. 2012. Silicification of the adaxial epidermis of leaves of a panicoid grass in relation to leaf position and section and environmental conditions. *Plant Biology* **14**: 596–604.

Gao X, Zou C, Wang L, Zhang F. 2006. Silicon decreases transpiration rate and conductance from stomata of maize plants. *Journal of Plant Nutrition* **29**: 1637–1647.

Garbuzov M, Reidinger S, Hartley SE. 2011. Interactive effects of plant-available soil silicon and herbivory on competition between two grass species. *Annals of Botany* **108**: 1355–1363.

Gocke M, Liang W, Sommer M, Kuzyakov Y. 2013. Silicon uptake by wheat: effects of Si pools and pH. *Journal of Plant Nutrition and Soil Science* **176**: 551–560.

Gong HJ, Chen KM, Chen GC, Wang SM, Zhang CL. 2003. Effects of silicon on growth of wheat under drought. *Journal of Plant Nutrition* **26**: 1055–1063.

Gu Y, Zhao Z, Pearsall DM. 2013. Phytolith morphology research on wild and domesticated rice species in East Asia. *Quaternary International* **287**: 141–148.

Guntzer F, Keller C, Meunier JD. 2012. Benefits of plan silicon for crops: a review. *Agronomy for a Sustainable Development* **32**: 201–213.

Hartley SE, Fitt RN, McLammon EL, Wade RN. 2015. Defending the leaf surface: intra- and inter-specific differences in silicon deposition in grasses in response to damage and silicon supply. *Frontiers in Plant Science* **6**: 35.

Hattori T, Inanaga S, Araki H, An P, Morita S, Luxová M, Lux A. 2005. Application of silicon enhanced drought tolerance in Sorghum bicolour. *Physiologia Plantarum* **123**: 459–466.

Henriet C, Bodarwé L, Dorel M, Draye X, Delvaux B. 2008. Leaf silicon content in banana (*Musa* spp.) reveals the weathering stage of volcanic ash soils in Guadeloupe. *Plant and Soil* **313**: 71–82.

Hodson MJ, Sangster AG. 1988. Observations on the distribution of mineral elements in the leaf of wheat (*Triticum aestivum* L.) with particular reference to silicon. *Annals of Botany* **62**: 463–471.

Hodson MJ, Sangster AG, Wynn Parry D. 1985. An ultrastructural study on the developmental phases and silicification of the glumes of *Phalaris canariensis* L. *Annals of Botany* **55**: 649–665.

Hodson MJ, White PJ, Mead A, Broadley MR. 2005. Phylogenetic variation in the silicon composition of plants. *Annals of Botany* **96**: 1027–1046.

Hutton JT, Norrish K. 1974. Silicon content of wheat husks in relation to water transpired. *Australian Journal of Agricultural Research* **25**: 203–212.

Issaharou-Matchi I, Barboni D, Meunier JD, Saadou M, Dussouillez P, Contoux C, Zirihi-Guede N. 2016. Intraspecific biogenic silica variations in the grass species *Pennisetum pedicellatum* along an evapotranspiration gradient in South Niger. *Flora* **220**: 84–93.

Jarvis SC. 1987. The uptake and transport of silicon by perennial ryegrass and wheat. *Plant and Soil* **97**: 429–437.

Johnson HB. 1975. Plant pubescence: an ecological perspective. *Botanical Review* **41**: 233–258.

Jones LHP, Handreck KA. 1965. Studies of silica in the oat plant. III. Uptake of silica from soils by the plant. *Plant and Soil* **23**: 79–96.

Kaplan L, Smith MB, Sneddon LA. 1992. Cereal grain phytoliths of Southwest Asia and Europe. In: Rapp G Jr, Mulholland SC, eds. *Phytolith systematics. Advances in archaeological and museum science, vol. 1*. New York, NY, USA: Plenum, 149–174.

Katz O, Lev-Yadum S, Bar P. 2013. Plasticity and variability in the patterns of phytolith formation in Asteraceae species along a large rainfall gradient in Israel. *Flora* **208**: 438–444.

Kaufman PB, Dayanandan P, Franklin CI, Takeoka Y. 1985. Structure and function of silica bodies in the epidermal system of grass shoots. *Annals of Botany* **55**: 487–507.

Kaufman PB, Dayanandan P, Takeoda Y, Bigelow WC, Jones JDD, Iler R. 1981. Silica in shoots of higher plants. In: Simpson TL, Volcani BE, eds. *Silicon and siliceous structures in biological systems*. New York, NY, USA: Springer, 409–449.

Kaufmann MR, Eckard AN. 1971. Evaluation of water stress control with polyethylene glycol by analysis of guttation. *Plant Physiology* **47**: 453–456.

Keller C, Rizwan M, Davidian JC, Pokrovsky OS, Bovet N, Chaurand P, Meunier JD. 2015. Effect of silicon on wheat seedlings (*Triticum turgidum* L.) grown in hydroponics and exposed to 0 to 30 µM Cu. *Planta* **241**: 847–860.

Liang Y, Nikolic M, Bélanger R, Gong H, Song A. 2015. *Silicon in agriculture: from theory to practice*. Dordrecht, the Netherlands: Springer Science+Business Media.

Ma JF. 2004. Role of silicon in enhancing the resistance of plants to biotic and abiotic stresses. *Soil Science and Plant Nutrition* **50**: 11–18.

Ma JF, Takahashi E. 2002. *Soil, fertilizer, and plant silicon research in Japan*. Amsterdam, the Netherlands: Elsevier.

Ma JF, Yamaji N. 2008. Functions and transport of silicon in plants. *Cellular and Molecular Life Science* **65**: 3049–3057.

Madella M, Alexandre A, Ball T, Grp IW. 2005. International code for phytolith nomenclature 1.0. *Annals of Botany* **96**: 253–260.

Mayland HF, Wright JL, Sojka RE. 1991. Silicon accumulation and water uptake by wheat. *Plant and Soil* **137**: 191–199.

McNaughton SJ, Tarrants JL, McNaughton MM, Davis RH. 1985. Silica as a defense against herbivory and a growth promotor in African grasses. *Ecology* **66**: 528–535.

Melzer SE, Knapp AK, Kirkman KP, Smith MD, Blair JM, Kelly EK. 2010. Fire and grazing impacts on silica production and storage in grass dominated ecosystems. *Biogeochemistry* **97**: 263–278.

Melzer SE, Knapp AK, Kirkman KP, Smith MD, Blair JB, Kelly EF. 2012. Fire and grazing impacts on silica production and storage in grass dominated ecosystems. *Biogeochemistry* **97**: 263–278.

LPED Lab. papers

Merah O, Deléens E, Monneveux P. 1999. Grain yield, carbon isotope discrimination, mineral and silicon content in durum wheat under different precipitation regimes. *Physiologia Plantarum* **107**: 387–394.

Meunier JD, Keller C, Guntzer F, Riotte J, Braun JJ, Anupama K. 2014. Assessment of the 1% Na_2CO_3 technique to quantify the phytolith pool. *Geoderma* **216**: 30–35.

Motomura H, Fujii T, Suzuki M. 2004. Silica deposition in relation to ageing of leaf tissues in *Sasa veitchii* (Carrière) Rehder (Poaceae: Bambusoideae). *Annals of Botany* **93**: 235–248.

Motomura H, Fujii T, Suzuki M. 2006. Silica deposition in abaxial epidermis before the opening of *Pleioblastus chino* (Poaceae, Bambusoideae). *Annals of Botany* **97**: 513–519.

Mulholland SC, Rapp G Jr. 1992. A morphological classification of grass silica-bodies. In: Rapp G Jr, Mulholland SC, eds. *Phytolith systematics. Advances in archaeological and museum science, vol. 1*. New York, NY, USA: Plenum, 65–89.

Novello A, Barboni D, Berti-Equille L, Mazur JC, Poilecot P, Vignaud P. 2012. Phytolith signal of aquatic plants and soils in Chad Central Africa. *Review of Palaeobotany and Palynology* **178**: 43–58.

Pei ZF, Ming DF, Liu D, Wan GL, Geng XX, Gong HJ, Zhou WJ. 2010. Silicon improves the tolerance to water-deficit stress induces by Polyethylene glycol in wheat (*Tricitum aestivum* L.) seedlings. *Journal of Plant Growth and Regulation* **29**: 106–115.

Quigley KM, Anderson TA. 2014. Leaf silica concentration in Serengeti grasses increases with watering but not clipping: insights from a common garden study and literature review. *Frontiers in Plant Science* **5**: 568.

Rizwan M, Ali S, Ibrahim M, Farid M, Adrees M, Bharwana SA, Zia-ur-Rehman M, Farooq Qayyum M, Abbas F. 2015. Mechanisms of silicon-mediated alleviation of drought stress in plants: a review. *Environmental Science and Pollution Research* **22**: 15416–15431.

Rizwan M, Meunier JD, Davidian JC, Pokrovsky OS, Bovet N, Keller K. 2016. Effects of silicon on growth and physiology of wheat seedlings (*Triticum turgidum* L. cv. Claudio) under Cd stress: a hydroponic study. *Environmental Science and Pollution Research* **23**: 1414–1427.

Rudall PJ, Prychid CJ, Gregory T. 2014. Epidermal patterning and silica phytoliths in grasses: an evolutionary history. *Botanical Review* **80**: 1–13.

Sacala E. 2009. Role of silicon in plant resistance to water stress. *Journal of Elementology* **14**: 619–630.

Samuels AL, Glass ADM, Ehret DL, Menzies JG. 1993. The effects of silicon supplementation on cucumber fruits: changes in surface characteristics. *Annals of Botany* **72**: 433–440.

Sandquist DR, Ehlinger JR. 1998. Intraspecific variation of drought adaptation in brittlebush: leaf pubescence and timing of leaf loss vary with rainfall. *Oecologia* **113**: 162–169.

Sangster AG, Hodson MJ, Parry DW, Rees JA. 1983. A developmental study of silicification in the trichomes and associated epidermal structures of the inflorescence bracts of the grass, *Phalaris canariensis* L. *Annals of Botany* **52**: 171–187.

Saud S, Li X, Chen Y, Zhang L, Fahad S, Hussain S, Sadiq A, Chen Y. 2014. Silicon application increases drought tolerance of Kentucky bluegrass by improving plant water relations and morphophysiological functions. *Scientific World Journal* **2014**: article ID 368694.

Shi Y, Zhang Y, Han W, Feng R, Hu Y, Guo J, Gong H. 2016. Silicon enhances water stress tolerance by improving root hydraulic conductance in *Solanum lycopersicum* l. *Frontiers in Plant Science* **7**: 196.

Soininen EM, Bråthen KA, Jusdado JGH, Reidinger S, Hartley SE. 2013. More than herbivory: levels of silica-based defences in grasses vary with plant species, genotype and location. *Oikos* **122**: 30–41.

Sonobe K, Hattori T, An P, Tsuji W, Aneji AE, Kobayashi S, Kawamura Y, Tanaka K, Inanaga S. 2011. Effect of silicon application on sorghum root. Responses to water stress. *Journal of Plant Nutrition* **34**: 71–82.

de Souza PV, Machado BR, da Silva DC, Menejes IPP, Araujo MS, de Jesus FG. 2014. Effect of resistance and trichome inducers on attraction of *Euschistus heros* (Hemiptera: Pentatomidae) to soybeans. *African Journal of Agricultural Research* **9**: 889–894.

Takeda HT, Ito F, Yamanaka S, Takiyama N, Yoshimo K. 2013. Roles of trichomes with silica particles on the surface of leaves in *Aphananthe aspera*. *AIP Advances* **3**: 032120.

Takeoka Y, Wada T, Naito K, Kaufman PB. 1984. Studies on silicification of epidermal tissues of grasses as investigated by solf X-ray image analysis. II. Differences in frequency of silica bodies in bulliform cells at different positions in the leaves of rice plants. *Japan Journal of Crop Science* **53**: 197–203.

Tubiello FN, Soussana JF, Howden SM. 2007. Crop and pasture response to climate change. *Proceedings of the National Academy of Sciences, USA* **104**: 19686–19690.

Twiss PC, Suess E, Smith RM. 1969. Morphological classification of grass phytoliths. *Soil Science Society of America Proceedings* **33**: 109–115.

Velde B, Barré P. 2010. *Soils, plants and clay minerals. Mineral and biologic interactions*. Berlin, Heidelberg, Germany: Springer.

Vijayakumari K, Puthur J. 2016. γ-Aminobutyric acid (GABA) priming enhances the osmotic stress tolerance in *Piper nigrum* Linn. Plants subjected to PEG-induced stress. *Plant Growth Regulation* **78**: 57–67.

Waterkeyn L, Bienfait A, Peeters A. 1982. Callose et silice epidermiques: rapports avec la transpiration cuticulaire. *Cellule* **73**: 267–287.

Weatherley PE. 1950. Studies in the water relations of the cotton plant. 1. The field measurement of water deficits in leaves. *New Phytologist* **49**: 81–97.

Wellso SG, Hoxie RP. 1982. The influence of environment on the expression of trichomes in wheat. *Crop Science* **22**: 879–886.

Whang SS, Kim K, Hess WM. 1998. Variation of silica bodies in leaf epidermal long cells within and among seventeen species of *Oryza* (Poaceae). *American Journal of Botany* **85**: 461–466.

Wynn Parry D, Smithson F. 1964. Types of opaline silica depositions in the leaves of british grasses. *Annals of Botany* **28**: 169–185.

Yoshida S, Ohnishi Y, Kitagishi K. 1962. Histochemistry of silicon in rice plant: III. The presence of cuticle-silica double layer in the epidermal tissue. *Soil Science and Plant Nutrition* **8**: 1–5.

Zhu Y, Gong H. 2014. Beneficial effects of silicon on salt and drought tolerance in plants. *Agronomy for a Sustainable Development* **34**: 455–472.

LPED Lab. papers